

Article

Characteristic Evaluation of Wind Power Distributed Generation Sizing in Distribution System

Issarachai Ngamroo, Wikorn Kotesakha, Suntiti Yoomak * and Aththapol Ngaopitakkul

School of Engineering, King Mongkut's Institute of Technology Ladkrabang, Bangkok 10520, Thailand

* Correspondence: suntiti.yo@kmitl.ac.th

Abstract: Energy consumption and environmental issues have become major drivers of increasing renewable energy penetration levels. The electricity generated from renewable energy sources is decentralized throughout distributed generation (DG), which is located at the distribution level. However, the presence of DG can change distribution system characteristics and affect protection systems. Thus, this study aims to investigate the impact of DG in term of its sizing and placement on distribution systems under both normal and fault conditions. In addition, the effects on voltage improvement under normal conditions and current under fault conditions are also considered. The case study system in this study was modelled after an actual section of a 22 kV distribution line from the Provincial Electricity Authority of Thailand using PSCAD software. For DG, wind turbine generation was selected as a renewable energy source. The simulation results demonstrated that the presence of DG has a significant impact on both voltage and current characteristics under both normal and fault conditions. These impacts on the distribution system caused by DG can affect the operation of conventional distribution systems, which require further analysis and preventive measures in order to ensure good system reliability.

Keywords: distributed generation; distribution system; voltage drop; fault; wind power generation



Citation: Ngamroo, I.; Kotesakha, W.; Yoomak, S.; Ngaopitakkul, A. Characteristic Evaluation of Wind Power Distributed Generation Sizing in Distribution System. *Sustainability* **2023**, *15*, 5581. <https://doi.org/10.3390/su15065581>

Academic Editor: Dalei Wang

Received: 14 February 2023

Revised: 20 March 2023

Accepted: 21 March 2023

Published: 22 March 2023



Copyright: © 2023 by the authors. Licensee MDPI, Basel, Switzerland. This article is an open access article distributed under the terms and conditions of the Creative Commons Attribution (CC BY) license (<https://creativecommons.org/licenses/by/4.0/>).

1. Introduction

Currently, energy and environmental problems have become major concerns in many countries because of the increasing consumption of fossil fuels and the corresponding release of greenhouse gases. In addition, populations and economies have been growing rapidly, which means that energy production cannot keep up with energy consumption rates. To address this, increasing energy production from renewable energy sources is among the methods that have gained attention from both governments and the private sector to replace the usage of fossil fuels. To achieve this goal, small-scale forms of renewable electric power generation called “distributed generation (DG)” systems must be adopted on a larger scale [1]. DG systems generate power from energy sources such as solar, wind, biomass, and biogas and are installed close to end users. In Thailand, the government plans to increase the proportion of energy generated from renewable energy sources by investing in renewable energy sources such as solar, wind, waste, biomass, and biogas in every region of the country that has potential for their use. In addition, the government has expanded its transmission and distribution system to keep up with increases in renewable energy penetration levels. According to data from the Ministry of Energy, Thailand created a long-term integration plan called The Power Development Plan (PDP2018 Revision 1) in 2018, which includes the objective of increasing renewable energy in power generation to 18.9% by 2037 [2]. The Alternative Energy Development Plan (AEDP2018) has the objective of increasing the proportion of renewable energy to 34.23% of total energy consumption by 2037. In particular, wind power generation will increase from 1102.82 MW in 2018 to 2989 MW in 2037, according to the plan [3]. This trend of rising DG penetration levels in the power system will affect the overall system characteristics in both positive and negative ways [4].

The connection of DG to the distribution system, including elements such as PV, thermal, wind, and water power plants, causes shifts in the characteristics of the power system [5–10]. Thus, the impacts of DG, both negative and positive, are reviewed in this paragraph. The conventional distribution system is a centralization generation (CG) type [5] with a large power generation unit that is placed near the energy source for generation and transmission of energy to customers through a distribution system. However, DG systems directly generate active power (P) [6] and reactive power (Q) [7] to the load customers via the distribution feeder. There are also side benefits of DG installations in distribution systems, such as voltage drop improvement [8], power loss reduction [9], improved power quality [10], and reactive power reduction. Literature reviews on DG placements in distribution systems and their effects on system characteristics [11–16] have been conducted. Optimal DG placement to improve voltage profiles and reduce power loss on distribution feeders in comparison to existing networks has also been studied [11]. In Ref. [12], the author proposed that DG placement along the distribution feeder impacts the bi-directional power flow of the distribution system. Various load characteristics were studied before determining the optimal DG placement and locating the weak bus of the primary feeder [13]. Furthermore, a technique to place DG to improve the power loss and reactive power compensation has been proposed [14]. Compared to the conventional technique, the results showed that DG installation achieved greater benefits, such as voltage drop improvement and an increase in the voltage profile. In addition, DG penetration with better allocation reduced the power loss of the system. In [15], the author reported that the voltage drop on the distribution line improved with the DG system, especially in the case of load unbalancing placement.

According to the above literature review, most DG systems can be improved through loss reductions and voltage deviations in the distribution system. These techniques have not been conducted for determining optimal locations to select the best position. Thus, DG placement techniques are proposed in [16–19]. DG placement techniques utilize the power loss and voltage profile. The DG placement technique has an impact on distribution feeders in term of voltage drop and power loss minimization, affecting the reliability of power systems [16]. In Ref. [17], studies were conducted regarding planning the optimal DG placement using the Strawberry Plant Propagation Algorithm (SPPA), which was applied on 33 and 69 nodes for testing. Ref. [18] studied the Meta-heuristics technique for optimal placements in multiple DG sizing variations, totaling 7 positions, which were performed on an IEEE 33-bus radial distribution system. Other devices that used capacitors were also proposed and placed on every weakness bus, using the analytical method technique for determining the optimal sizing and placement testing on the IEEE 37-bus [19].

Wind turbine generation (WTG) is one of the main types of DG that uses renewable energy sources that is on par with solar power systems. Past studies on the impacts of various WTG placements on distribution systems have been presented in [20,21]. The results indicated that operational issues that occur in systems with other types of DG also occur in the case of wind farm projects. Various phase faults in a distribution system consisting of wind power generation that uses a doubly fed induction generator (DFIG) can affect relay operation and are caused by a malfunction in a conventional directional relay. Research on a new approach to fault classification also demonstrated the effect of DFIG on the wave shape of the fault current, as can be seen in [22,23]. A smart grid system with a high level of renewable energy penetration, especially in wind farms, requires accurate and rapid fault location algorithms to prevent any tripping out of wind power generators [24]. Moreover, the fault current on the distribution system will be more affected by the installed WTG according to parameters such as sizing and placement [25]. To determine the type of fault and identify the fault line, simulation programs have been utilized to determine the correct location [26]. In addition, fault currents have been monitored from the load side and fault point occurrence to improve the relay-setting coordination along with the distribution system. The fault current will increase in the system depending on the DG installation size [27,28]. The reason for this is the penetration of DG, which injects continuous current

into the system when the fault is still occurring. The WTG still provides power under fault conditions through the distribution system because the wind power comes from the flow of wind speed, which drives the mechanisms of the wind turbine and generates power regardless of whether a fault occurs on the distribution line [29]. In [30], the researcher employed the reduction amplitude method when the fault occurred through fault current limiter (FCL) installation to the distribution system. Thus, the sizing and placement of the DG were optimized to avoid high FLC sizing selection.

In [31–35], research on the impact of DG placement on distribution systems when various faults occur was conducted. The optimal DG placement was determined based on the right placement location and sizing of the DG [31]. Investigations analyzing the root causes of DG integration in a distribution system used for resetting relay protection have also been conducted [32,33]. In [34], the authors proposed the optimal placement of fault detection for identifying the zone of the fault location along with the distribution system, and the results could be used to improve the reliability of the system. Furthermore, DG causes significant changes in various aspects of the power system characteristics when connected to the system in both steady and transient states. In addition, the DG placement on the distribution system must consider the fault occurrence among the feeders to identify and determine the fault location, thus helping to minimize the major fault occurrences in the distribution system [35]. Ref. [36] determined the various DG types to connect with the grid for monitoring performance.

From the literature review it can be seen that the integration of DG has various impacts on conventional distribution systems. However, many research articles focused on case studies with fixed DG sizes and locations. Thus, this paper aims to present the effect of DG on various parameters such as voltage under normal conditions and system currents during fault conditions. The case study distribution system using a 22-kV distribution network located in the northern part of Thailand's central region was simulated using PSCAD software. The evaluation of system characteristics considered various factors such as DG location, number of DGs, and fault locations in consideration. Various case studies have been conducted in order to anticipate the system behavior in case of an increase in the penetration level on the distribution line and to analyze the trend to ensure that the traditional distribution system can operate under the new condition reliability.

The contribution of this study as follows:

- The case study replicated an actual distribution line from the Provincial Electricity Authority (PEA) 22 kV distribution network, which represents real load and connection;
- The voltage characteristic under a normal condition and the side benefits of DG installation on the distribution in terms of voltage drop improvement were analyzed using various DG sizes, numbers, and locations;
- The current characteristic of the distribution system with various cases of DG installations under fault occurrences were also observed.

The results from this study can be used to anticipate both the positive effects (in terms of improving the voltage drop) and negative effects (in terms of its impact on the current characteristics of the system) of DG implementation, which can help ensure reliable operation of the distribution system with higher distributed generator penetration.

The remainder of this paper can be divided into the following sections. Section 2 provides details and a configuration of the distribution system used in the case study. The results in terms of voltage improvement obtained by using DG are presented in Section 3. Section 4 evaluates the impact of fault conditions on the distribution system characteristics under different DG conditions. Finally, the findings of the study are summarized and discussed in the conclusion.

2. Case Study Distribution System

The characteristics of the distribution system used in the case study were modelled after the actual PEA 22-kV distribution line connected between the Sukhothai (STA) and Sawankhalok (SWA) substations in the northern region of Thailand. The distance between

the substations is 43 km, and the configuration of the cable in this section of the distribution line is summarized in Table 1.

Table 1. Configuration of the case study distribution system.

Parameters	Configurations
1. Rated voltage (V_{L-L}, V_{rms})	22 kV
2. Boundary voltage	20.9–23.1 kV
3. Lean conductor	3 conductors
■ SAC cable	185 mm ²
■ Outer diameter	0.00799 m
■ DC resistance	0.164 Ω
4. Distribution line length	43 km
5. Total loads	9 loads
6. PF loads	0.95

The parameters of each customer load on the distribution system are summarized in Table 2. The customer load requirement in this section was 23.59 MVA with an average power factor of 0.95, which can be simplified into nine connected points along a 43 km distribution line. The largest load was number 4, located 27.5 km from the STA substation, and the smallest load was number 9, located 37.5 km from the STA substation.

Table 2. Parameters of the interconnected load in the distribution system.

Load No.	Distance (STA–Load) (km)	Apparent Power (MVA)	PF.
1	5.5	0.86	0.95
2	10	4.71	0.95
3	14.5	2.55	0.95
4	17.5	6.02	0.95
5	20	2.97	0.95
6	26	0.97	0.95
7	30.5	2.36	0.95
8	33.5	2.96	0.95
9	37.5	0.19	0.95
		23.59 MVA	

The distribution line used as a case study can be represented by a single-line diagram, as shown in Figure 1. In Figure 1a, the simplified diagram consists of nine connected loads with varying power demands, with the largest connected load of 6.02 MVA located at bus No. 4, slightly near the STA substation. The PSCAD diagram is illustrated in Figure 1b, where the substation is replaced with a voltage source and the load is connected to the transmission line model with a bus, circuit breaker, and measurement device.

To evaluate the characteristics of the distribution system used in the case study, a simulation using PSCAD software was performed. System parameters such as voltage and current were obtained through measurement devices installed on the substation and each load bus. The three-phase voltage waveform obtained in front of the STA and SWA substation displayed in Figure 2 shows the sinusoidal wave characteristic with each phase according to 120°, which is common in alternate current systems. For the load parameter, the obtained results are summarized in Table 3. The voltage level on the load bus decreased as the distance between the load bus and the substation increased. This resulted from

the voltage drop on the load and cable as power was fed along the distribution line. The voltage was the lowest on load No. 4, which was also the largest load on the distribution line and was located farthest from both substations. On the other hand, the current from both substations was a combination of the current that flowed through each load, and the amplitude depended on the sizing of the load, which was highest for load No.4. The current on the STA substation was higher than that on the SWA because the sizing of the load near the STA substation was larger than that near the SWA substation. Thus, a larger amount of power was fed from the STA substation.

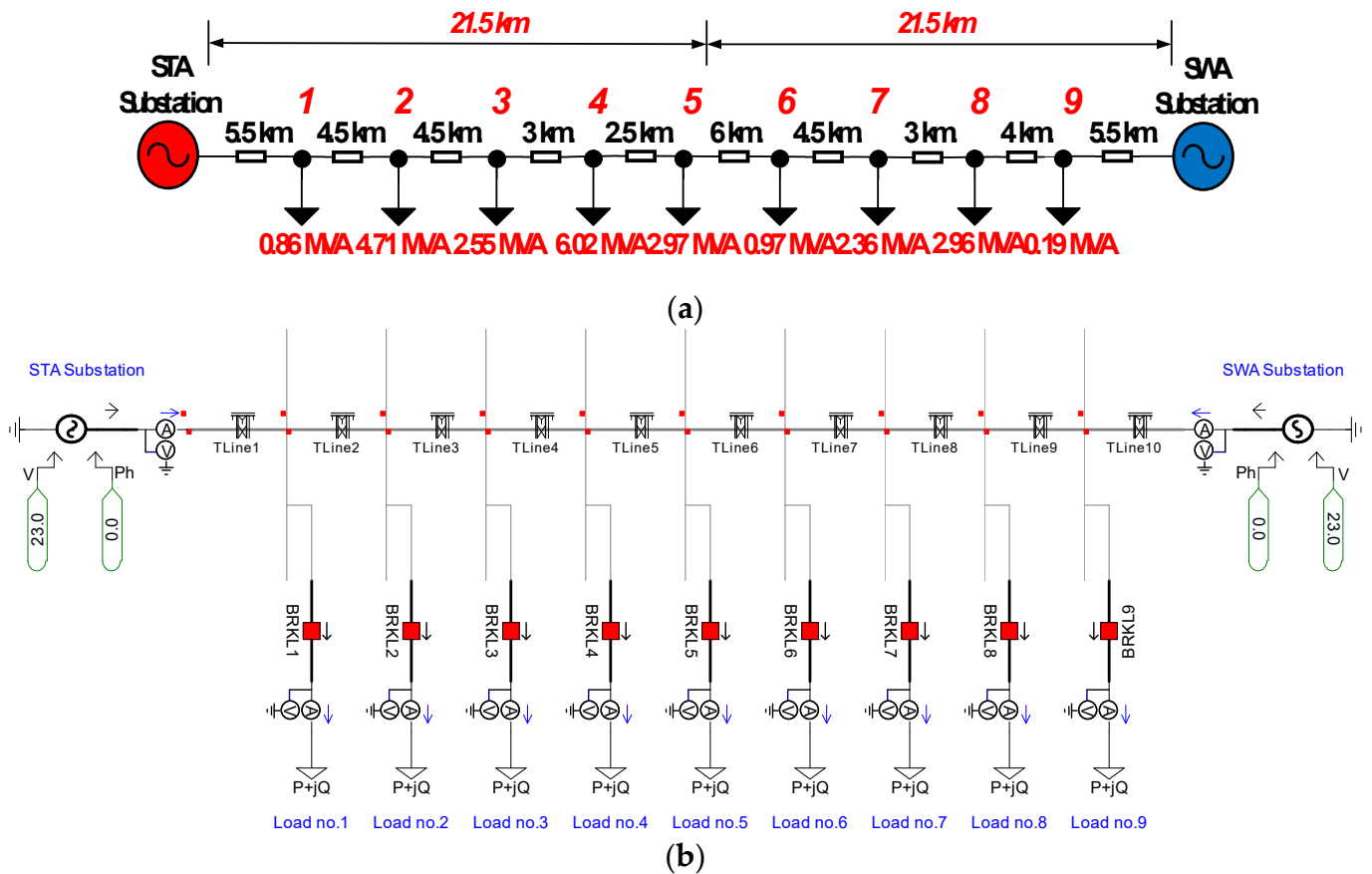


Figure 1. The 22 kV distribution system used in the case study. (a) Single-line diagram; (b) PSCAD diagram.

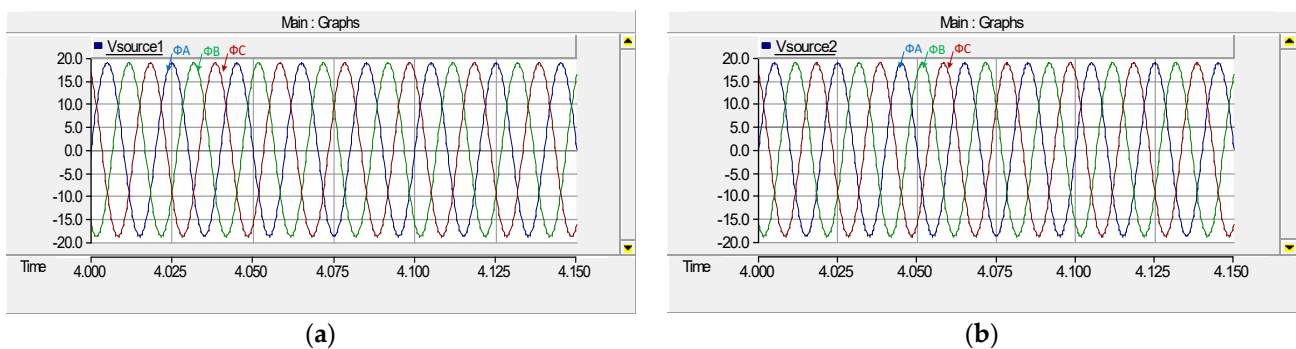
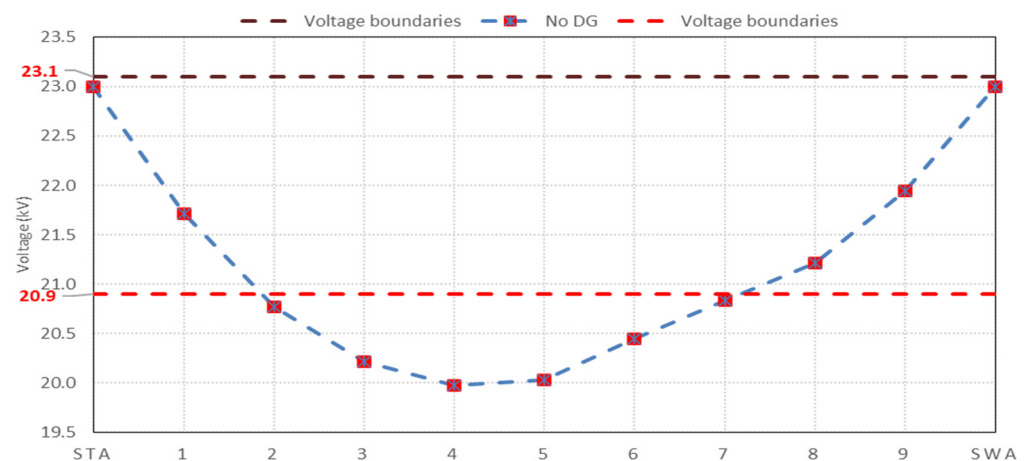


Figure 2. Three-phase voltage waveform in case study distribution system. (a) STA substation; (b) SWA substation.

Table 3. Parameter results of base case (no DG) simulation.

Descriptions	Parameters Recorded					
	V (kV)	I (kA)	P (MW)	Q (MVA _r)	S (MVA)	
STA (S1)	23.000000	0.499433	19.174202	8.096472	20.813526	
Load No. 1	21.705532	0.035279	1.255549	0.427419	1.326307	
Load No. 2	20.766570	0.184679	6.308891	2.078501	6.642459	
Load No. 3	20.213322	0.097514	3.243475	1.065713	3.414070	
Load No. 4	19.967074	0.226968	7.460242	2.441514	7.849598	
Measuring Points	Load No. 5	20.017326	0.112525	3.703464	1.226886	3.901396
	Load No. 6	20.433511	0.037232	1.254766	0.402474	1.317734
	Load No. 7	20.821111	0.093333	3.195578	1.056986	3.365848
	Load No. 8	21.203214	0.118314	4.129579	1.351087	4.344980
	Load No. 9	21.939189	0.007498	0.272923	0.081175	0.284739
SWA (S2)	23.000000	0.413103	15.078666	6.592662	16.456894	

From a voltage perspective, the voltage drop level that occurred on the distribution line is significant because of its impact on the end user. The PEA has set a standard that regulates the voltage level, which should not exceed 5% of that of the substation. The voltage level of the 22-kV case study distribution system is plotted in comparison with the PEA standard, as shown in Figure 3. The 5% voltage boundaries are 23.1 kV and 20.9 kV for the upper and lower boundaries of the PEA standard, respectively. From the figure, it can be seen that the voltages on the bus nos. 2 through nos. 7 were lower than the minimum imposed by the standard.

**Figure 3.** Voltage level of the case study distribution system.

This under-voltage issue on the majority of the load can impact end users on this specific distribution line. However, the presence of DG at the distribution level may be able to improve the voltage level on the distribution line. Thus, a characteristic evaluation of the distribution system with a connected wind-type DG under different conditions, particularly at the voltage level, is presented in the next section.

3. Distribution System with Distributed Generation

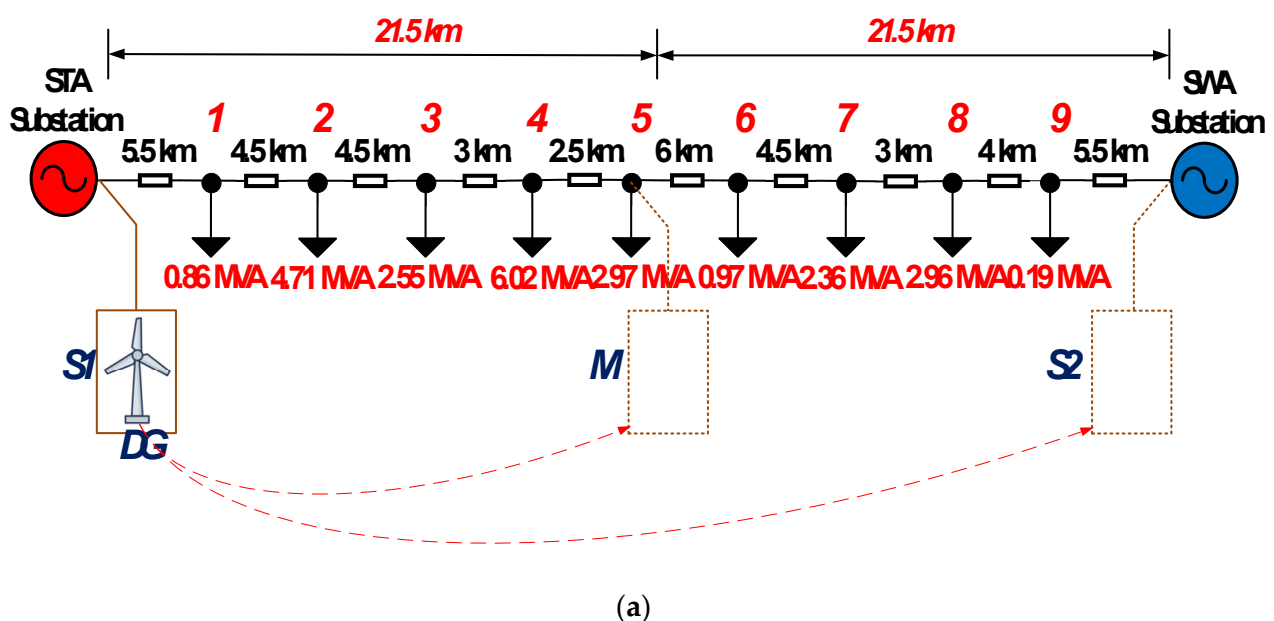
In this case study, WTG was selected as the type of DG to be connected to a distribution system. The diagrams of the wind turbine model and its PSCAD counterpart used in the case study are illustrated as shown in Figure 4a,b, respectively. The WTG components consist of a wind source (point 1), which can be used to control the input wind speed for

Table 4. WTG parameters used in the case study.

Components	Parameters	Configurations
1. Wind Source	Average wind Speed (m/s)	6
	Generator rated (MVA)	2
2. Wind Turbine Generator	Rotor radius (m)	43.5
	Rotor area (m ²)	5944
	Air density (kg/m ³)	1.225
	Rate voltage per phase (kV)	0.398
3. Synchronous Machine	Rate current (kA)	1.840
	Frequency (Hz)	50
	Frequency (Hz)	50
4. Unit Transformer	Apparent power (MVA)	2
	Primary voltage (kV)	0.690
	Secondary voltage (kV)	22

From Table 4, the average wind speed at the case study location was 6 m/s. The parameters of the generator in the turbine had a rated power of 2 MVA, mechanical speed of 16.667 Hz, rotor diameter of 43.5 m, and air density of 1.225 kg/m³. The generator type was synchronous with a rated configuration voltage of 0.398 kV and 1.84 kA and a power converter control frequency for synchronization to the grid at 50 Hz. The power transformer was a step-up voltage Delta-Wye connection with a voltage ratio of 0.69/22 kV connected between the WTG and the distribution line.

The DG placement consisted of three main locations: near the STA substation (S1), on the middle point of the distribution line (M), and near the SWA substation (S2). Moreover, the sizing of the WTG varied from 2 MW to 8 MW, which is the maximum allowable DG output to connect with the grid according to PEA regulations. A simplified diagram of the case study distribution system with the WTG is shown in Figure 5a,b, which show a diagram from PSCAD software. The simulation results from PSCAD with different DG sizing and placement are discussed in the next section.

**Figure 5.** Cont.

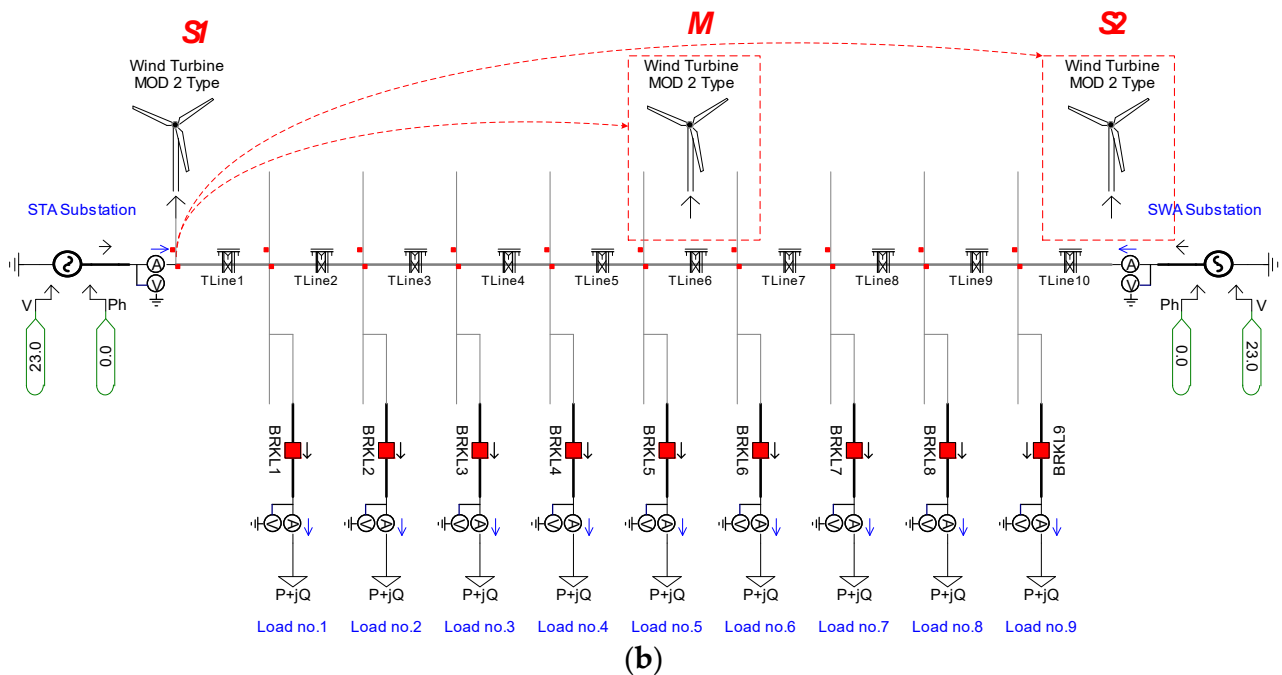
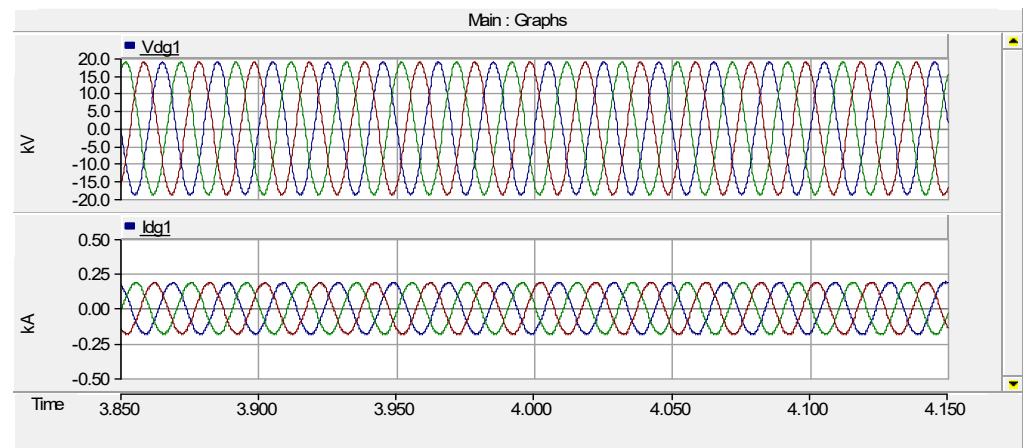


Figure 5. Case study diagram with single DG placement on the distribution system. (a) Single-line diagram; (b) PSCAD model.

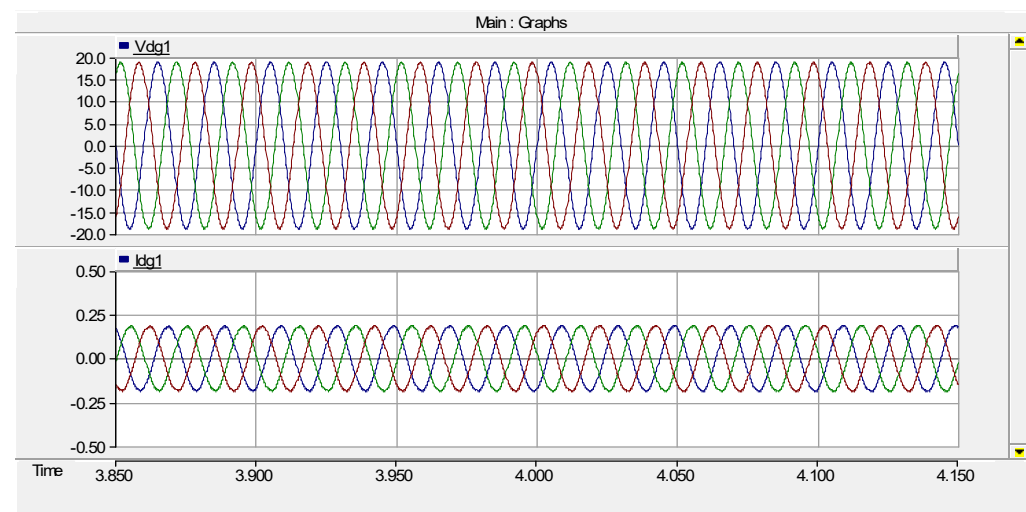
3.1. Distribution Characteristics in the Case of a Single 2 MW DG with Different Placement

The evaluation of distribution characteristics with different DG placements was conducted by simulating a 2 MW DG at three different positions. The selected positions consisted of the STA substation, the middle of the distribution line, and the SWA substation. The simulation results in terms of sinusoidal voltage and current waveform for the three different DG placements are shown in Figure 6. The amplitude of both the sinusoidal voltage and current waveform from the STA substation (Figure 6a) were similar to those of the substation (Figure 6b) and those of the case without DG (Figure 2). This result is due to the DG installed on the substation bus, where the voltage level is constant. On the other hand, DG placement at the middle of the distribution line (Figure 6c) had a lower peak-to-peak voltage compared to the substation placement because of the voltage drop that occurred on the distribution line. For the current waveform, the amplitude depended on the power provided by the DG sizing.

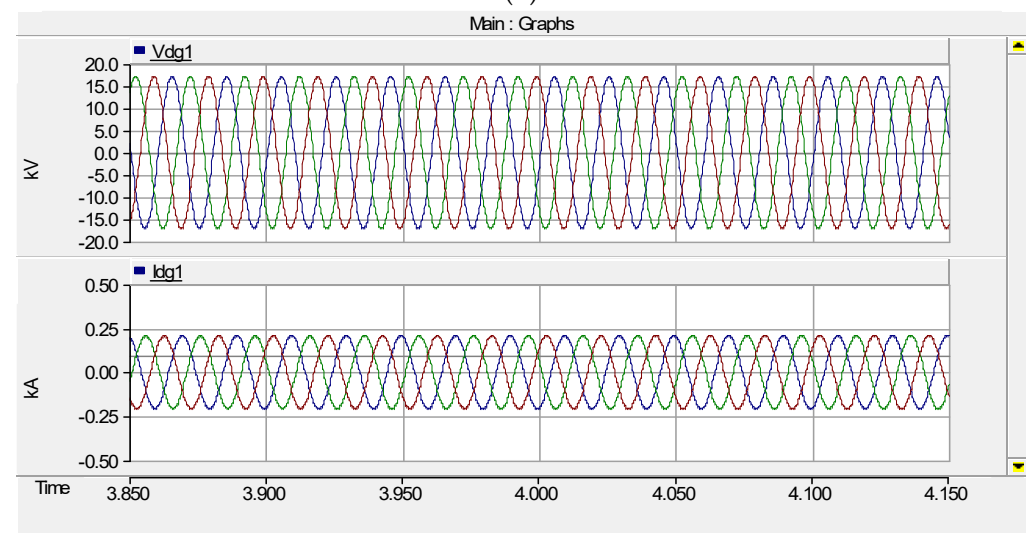
The obtained current and voltage of each measuring point from three different 2 MW DG placement locations in comparison with the case without DG are summarized in Table 5. With respect to the voltage level, the RMS voltages at each measurement point in the cases of DG placement near both substations were similar to that in the base case without DG. This results from the constant voltage level on the substation bus; therefore, the DG does not have an effect on the voltage. In the case of DG placement in the middle of the distribution line, the RMS voltages on each load bus increased compared to those in the base case. This is because DG provides power to the nearest load instead of power feeding from the substation, resulting in a reduction in the voltage drop. For the current, the DG had an impact on the current level by feeding power to the nearest load instead of the substation. Thus, the current level of a substation reduced when DG placement was near it compared with the base case without DG. However, the sizing of DG was small in comparison to the load, and the effect did not reach the substation on the other side. When the DG was placed in the middle of the distribution line, the additional power generated from the DG resulted in an increase in the current level on the nearest load and a reduction in the substation current level.



(a)



(b)



(c)

Figure 6. Sinusoidal voltage and current waveform for distribution system with 2 MW DG placement. (a) DG placement near STA substation; (b) DG placement near SWA substation; (c) DG placement in middle of distribution line.

Table 5. Simulation results for single 2 MW DG with different placements.

Items	Measuring Points	Descriptions							
		Base Case (No DG)	Near STA Substation (DG-STA)	On the Middle Point of the Distribution Line (DG-Middle)	Near SWA Substation (DG-SWA)	Base Case (No DG)	Near STA Substation (DG-STA)	On the Middle Point of the Distribution Line (DG-Middle)	Near SWA Substation (DG-SWA)
Voltage (kV)				Current (kA)					
1	STA (S1)	23.000000	23.000000	23.000000	23.000000	0.499433	0.411413	0.468915	0.499443
2	Load No. 1	21.705532	21.705543	21.908088	21.705561	0.035279	0.035279	0.035607	0.035279
3	Load No. 2	20.766570	20.766675	21.138453	20.766642	0.184679	0.184673	0.187696	0.184673
4	Load No. 3	20.213322	20.213380	20.761723	20.213555	0.097514	0.097515	0.100147	0.097515
5	Load No. 4	19.967074	19.967146	20.639817	19.967360	0.226968	0.226969	0.234555	0.226972
6	Load No. 5	20.017326	20.017389	20.798338	20.017638	0.112525	0.112525	0.116922	0.112526
7	Load No. 6	20.433511	20.433512	21.099504	20.433847	0.037232	0.037232	0.038440	0.037233
8	Load No. 7	20.821111	20.821148	21.300304	20.821548	0.093333	0.093333	0.095484	0.093335
9	Load No. 8	21.203214	21.203240	21.563076	21.203488	0.118314	0.118314	0.120318	0.118316
10	Load No. 9	21.939189	21.939206	22.146445	21.939720	0.007498	0.007498	0.007569	0.007498
11	SWA (S2)	23.000000	23.000000	23.000000	23.000000	0.413103	0.413099	0.381220	0.330026

The voltage level at each measurement point was plotted in the voltage profile along the distribution line in comparison with the voltage regulation, as shown in Figure 7. The PEA standards of maximum and minimum voltage levels indicated that under normal conditions, the 22 kV system had an upper voltage boundary of 23.1 kV and a lower voltage boundary of 20.90 kV. From the figure, the distribution system without DG had voltage levels on loads 2 through 7 that were lower than the minimum regulation boundary. Although the voltage level improved in the case of DG placement in the middle of the distribution line, the voltage levels on loads 3 through 5 were still lower than the minimum regulation boundary. However, the PEA interconnection code allows up to 8 MW of a DG unit to be connected to a single bus. Thus, the evaluation of different DG sizing and the corresponding effects in cases where the penetration level is higher than 2 MW were performed.

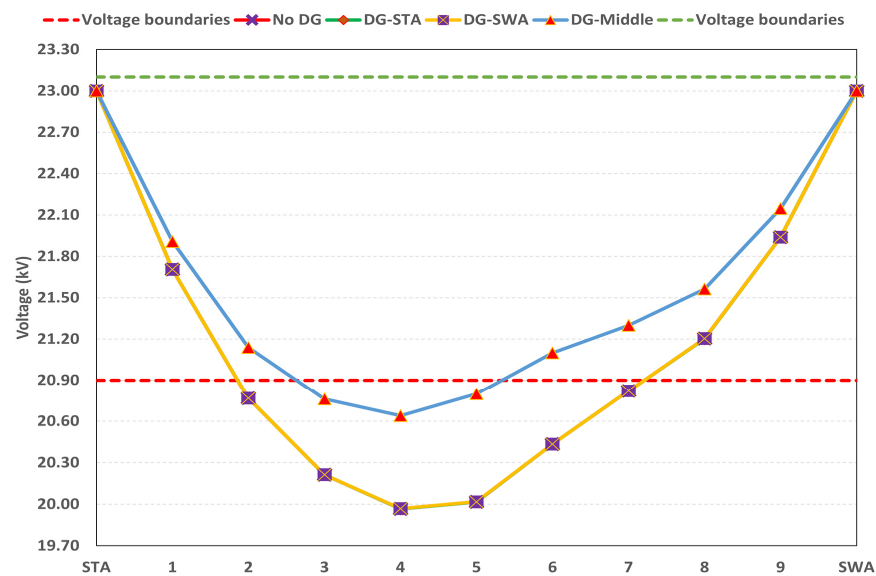


Figure 7. Voltage profile of the distribution system with different 2 MW DG placements.

3.2. Characteristics of Voltages in the Case of Varying DG Sizing

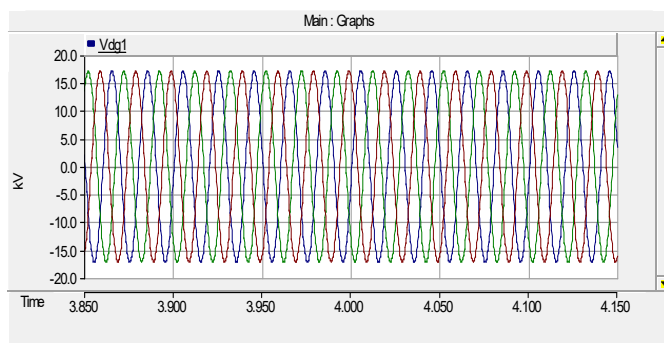
From a previous case study, only the case of DG placement in the middle of the distribution line showed results in terms of voltage improvement on load buses. Thus, this section will focus only on the case of DG placement at the middle of the distribution line and varied sizing from 2 MW to 8 MW. The voltage levels when the DG sizing varied are summarized in Table 6. The RMS voltage level loads increased in comparison with that of the distribution system without DG and the voltage increased as the DG sizing increased. As for the voltage regulation, the DG size of 3 MW at the middle of the distribution line had a voltage level at all load buses higher than the lower boundary of voltage regulation. This is because the DG was located near the load and provided power to the load instead of to the substation. Thus, there was a smaller voltage drop from the distance of the load to the substation. For the sinusoidal voltage waveform, the voltage amplitude at the connected point increased depending on DG sizing, as shown in Figure 8.

Table 6. The voltage results in the case of 2 MW to 8 MW DG placement at the middle of the distribution line (M).

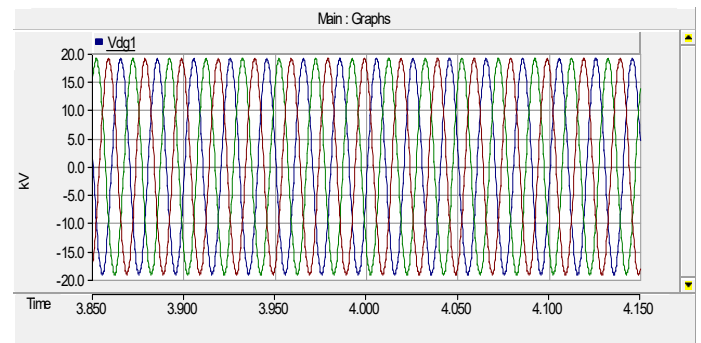
Single DG Sizing	Measuring Points										
	STA	1	2	3	4	5	6	7	8	9	SWA
no DG	23.000000	21.705532	20.766570	20.213322	19.967074	20.017326	20.433511	20.821111	21.203214	21.939189	23.000000
2 MW	23.000000	21.908088	21.138453	20.761723	20.639817	20.798338	21.099504	21.300304	21.563076	22.146445	23.000000

Table 6. Cont.

Single DG Sizing	Measuring Points										
	STA	1	2	3	4	5	6	7	8	9	SWA
3 MW	23.000000	21.974048	21.293040	21.025706	21.006142	21.222554	21.392216	21.504872	21.748671	22.239908	23.000000
4 MW	23.000000	22.107511	21.482672	21.272889	21.265034	21.525231	21.713015	21.746262	21.901710	22.342198	23.000000
5 MW	23.000000	22.184035	21.632193	21.489586	21.586236	21.854500	21.990732	21.959655	22.061591	22.433231	23.000000
6 MW	23.000000	22.281338	21.807338	21.751126	21.856676	22.217459	22.299483	22.176007	22.216389	22.524413	23.000000
7 MW	23.000000	22.333308	21.990926	21.964674	22.105478	22.554267	22.567886	22.367582	22.380118	22.614138	23.000000
8 MW	23.000000	22.441116	22.105417	22.191798	22.397389	22.855555	22.834169	22.547406	22.504952	22.688590	23.000000



(a)



(b)

Figure 8. The sinusoidal voltage waveform in the case of DG connected at the middle of the distribution line. (a) 2 MW DG; (b) 8 MW DG.

The voltage characteristics of each case study compared with the PEA voltage regulation are summarized in Figure 9. The voltage levels on all load buses increased as the DG sizing increased from 2 MW to 8 MW. The DG installation was located in the middle of the transmission line, that is, between buses 5 and 6. This resulted in the voltage level in these two buses being higher than the other buses because of the proximity of the DG. At the maximum connected DG allowance of 8 MW, the voltage level did not exceed the upper boundary of the PEA voltage regulation. This change in distribution system characteristics represents a positive effect. However, the change in current characteristics under normal conditions due to DG can impact the system, especially under fault conditions. Thus, the next section discusses the impact of DG on the distribution system under fault conditions.

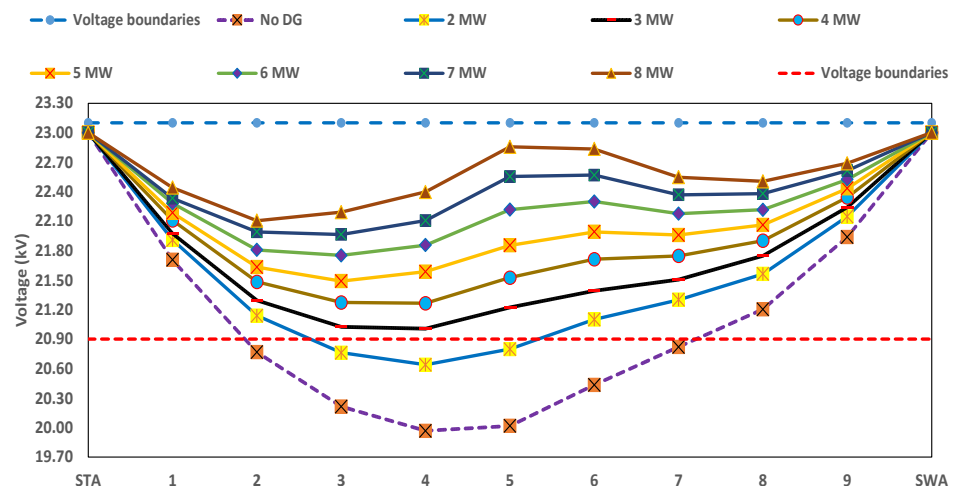


Figure 9. The voltage profile of DG placement at the middle position of the distribution line.

4. Distribution System with Distributed Generation in the Case of Fault Occurrence

The simulation results under normal conditions show that DG interconnected into a distribution system can indeed alter the system characteristics by increasing the voltage level along the distribution line. However, the characteristics of the system under fault conditions may be affected by the presence of DG. Thus, an evaluation of a system with DG under fault conditions must be performed.

4.1. Distribution System in the Case without dg under Fault Conditions

To evaluate the characteristics under fault conditions, a case study distribution system without DG was simulated. The location of the fault was varied across six different locations: L1 at 5.5 km, L2 at 10 km, L3 at 17.5 km (on the bus connected with load No. 4), L4 at 20 km (middle point), L5 at 33.5 km (10 km from SWA substation), and L6 at 37.5 km (5.5 km from the SWA substation). The single-line diagram of the distribution system under fault conditions and its PSCAD counterpart are shown in Figure 10a,b, respectively.

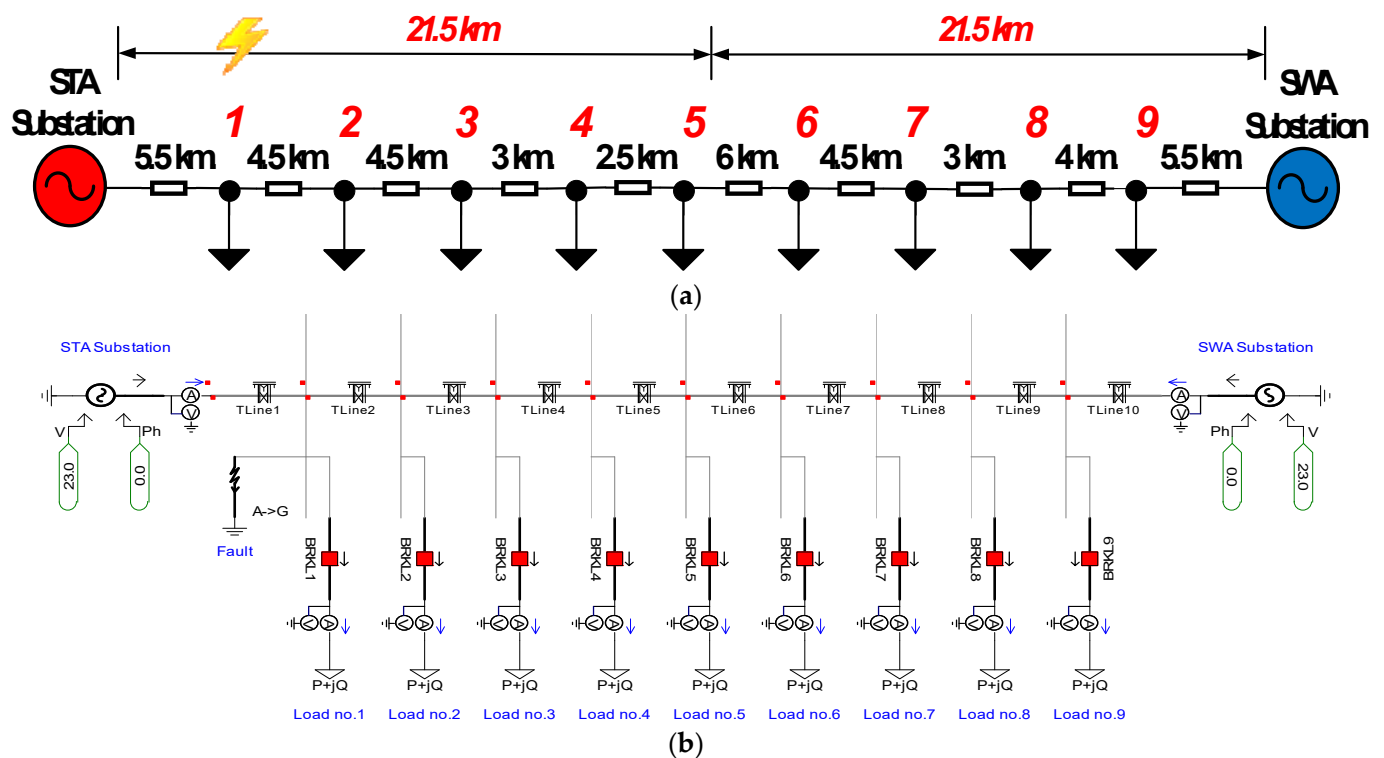


Figure 10. Distribution system without DG under fault condition. (a) Single-line diagram; (b) PSCAD diagram.

The sinusoidal current waveforms at the STA and SWA substations under normal conditions are displayed in Figure 11a,b, respectively. The different amplitudes obtained from the load sizing on the STA side were larger than those on the SWA side. Thus, the STA substation needed to provide more power, which resulted in a higher current amplitude compared to that of the SWA substation. Under the fault condition at L1, the single line to ground fault in Figure 11c shows that the fault phase current from the STA was significantly higher than that of the other phases, and it was also higher than the fault phase measured from the SWA side because the fault location was near the STA substation. For the three-phase fault in Figure 11d, the currents from both the STA and SWA in all phases had similar characteristics that were significantly higher than under pre-fault conditions. However, the current from the STA substation was higher than that from the SWA substation because the location of the fault was similar to that of the case with single-phase to ground fault.

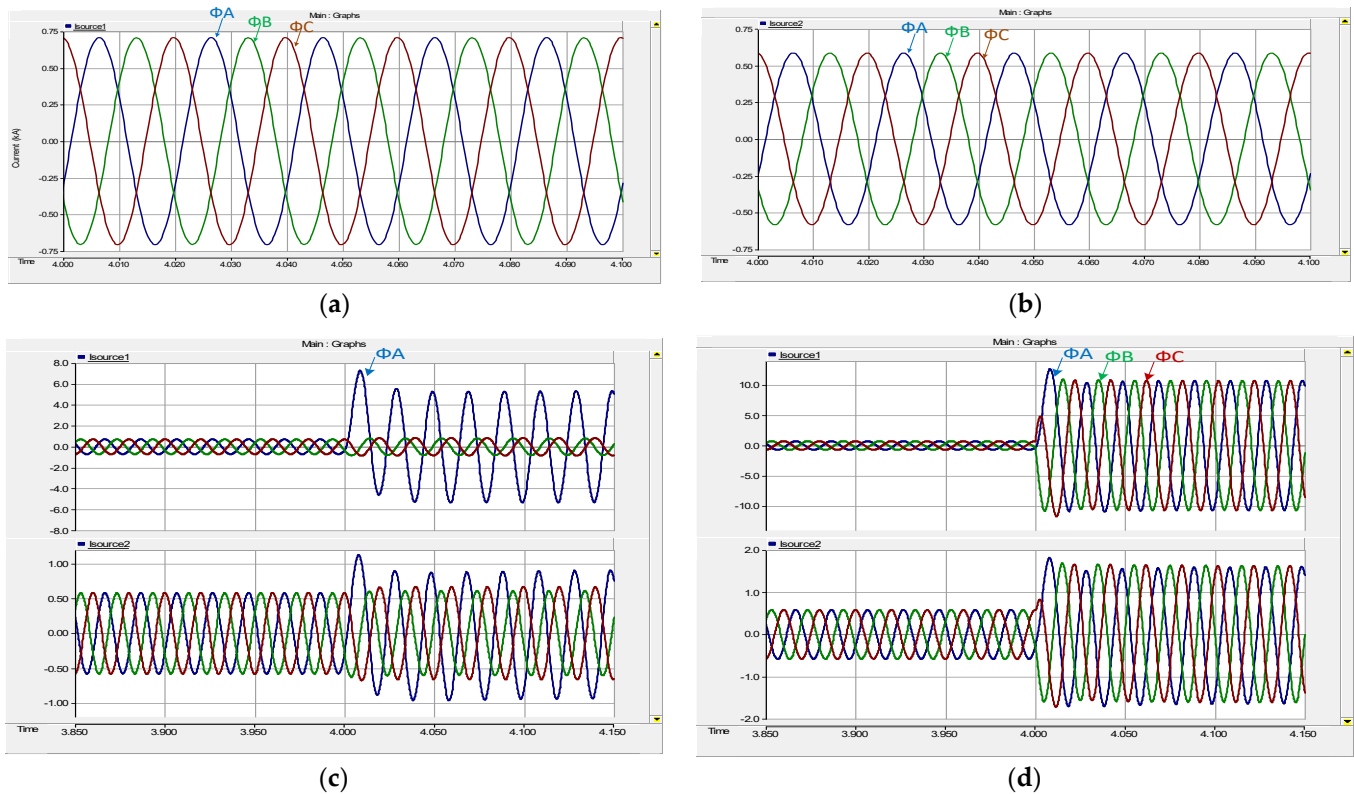


Figure 11. Normal and fault condition waveforms without DG. (a) STA substation current waveform; (b) SWA substation current waveform; (c) Single-phase to ground fault; (d) Three-phase to ground fault.

The currents measured from all buses during the fault conditions are listed in Table 7. Considering that phase-A-to-ground faults occur at L1, the magnitudes of current phase A on both substations were higher than those of other phases because the current from the substation flowed directly to the fault location, which had a lower resistance path. In addition, current phase A on the other load bus decreased compared to that in the normal condition because the current flowed to the fault location instead of the load. At the same time, the currents of the B and C phases could feed to the loads as before, but the current magnitude shifted to be slightly higher compared to that with normal conditions because of the unbalanced substation current. However, the current gap between the fault and normal conditions on load bus decreased as the fault location moved away from the observed load bus. When comparing the current from the STA and SWA substations, the current on the STA substation was significantly higher than that on the SWA substation because the fault was located nearby. In the case of a varied fault location away from L1, the current from the STA decreased as the distance increased. The fault current was the lowest around location L4, owing to the distance from the substation. Conversely, when the fault location moved nearer to the SWA substation, the current increased significantly.

Comparing the pre- and post-fault conditions shows that the fault currents of the STA and SWA substations increased under fault conditions. This increase depended on the distance between the fault location and the substation. However, this characteristic may change when the distribution system has a DG connection, which can act as an additional generating source.

Table 7. Simulation results in the case of fault occurrences in the system without DG.

Fault Location	Parameters		Measuring Points										
			STA (S1)	Load No. 1	Load No. 2	Load No. 3	Load No. 4	Load No. 5	Load No. 6	Load No. 7	Load No. 8	Load No. 9	SWA (S2)
Normal Condition	RMS current (kA)	A	0.499433	0.035279	0.184679	0.097514	0.226968	0.112525	0.037232	0.093333	0.118314	0.007498	0.413103
		B	0.499433	0.035279	0.184679	0.097514	0.226968	0.112525	0.037232	0.093333	0.118314	0.007498	0.413103
		C	0.499433	0.035279	0.184679	0.097514	0.226968	0.112525	0.037232	0.093333	0.118314	0.007498	0.413103
Fault at 5.5 km (L1)	RMS current (kA)	A	3.425437	3.80059	0.045354	0.034836	0.104118	0.059266	0.025076	0.072426	0.098934	0.006807	0.656846
		B	0.570717	0.048403	0.227256	0.110387	0.244291	0.118632	0.037849	0.093260	0.11784	0.00748	0.431361
		C	0.60103	0.045938	0.231498	0.118328	0.270682	0.131697	0.041878	0.101779	0.1262	0.00778	0.470331
Fault at 10 km (L2)	RMS current (kA)	A	2.039706	0.018407	2.534366	0.025607	0.075196	0.046396	0.022077	0.067126	0.094045	0.006635	0.736406
		B	0.584159	0.040447	0.242797	0.115761	0.253281	0.122223	0.038493	0.094094	0.118467	0.007506	0.444318
		C	0.612174	0.040432	0.239505	0.12189	0.278379	0.135086	0.04227	0.103318	0.127651	0.007829	0.479773
Fault at 17.5 km (L3)	RMS current (kA)	A	1.28695	0.02593	0.092053	0.031512	1.979025	0.031697	0.015228	0.05431	0.081949	0.006207	0.920934
		B	0.576755	0.036578	0.200288	0.11494	0.287371	0.136297	0.041345	0.098378	0.122088	0.007624	0.462517
		C	0.607462	0.038518	0.21505	0.121232	0.294322	0.141964	0.044407	0.106478	0.130603	0.007931	0.490508
Fault at 20 km (L4)	RMS Current (kA)	A	1.144118	0.027471	0.107245	0.035007	0.056589	1.880047	0.014092	0.049399	0.076969	0.006017	0.990623
		B	0.562203	0.036117	0.195049	0.109855	0.27104	0.14385	0.042907	0.100751	0.124109	0.007693	0.46411
		C	0.598486	0.037899	0.21074	0.117767	0.28416	0.14591	0.045309	0.108073	0.132065	0.00798	0.489472
Fault at 33.5 km (L5)	RMS Current (kA)	A	0.786051	0.031503	0.146545	0.066019	0.133924	0.057004	0.011675	0.026774	2.513962	0.003605	2.065382
		B	0.527778	0.035217	0.184619	0.099259	0.236191	0.12059	0.044063	0.118574	0.158727	0.008857	0.474618
		C	0.56739	0.036791	0.199489	0.10909	0.259745	0.131519	0.045305	0.118059	0.154326	0.00866	0.488163
Fault at 37.5 km (L6)	RMS current (kA)	A	0.728949	0.032086	0.152416	0.07073	0.147694	0.065068	0.014511	0.025329	0.028757	3.713365	3.355621
		B	0.518104	0.035196	0.184339	0.0987	0.233933	0.118883	0.042851	0.114254	0.151947	0.101409	0.469314
		C	0.558022	0.036599	0.197586	0.107615	0.255573	0.129131	0.044292	0.114906	0.149521	0.009837	0.481258

4.2. Distribution System in the Case of Single DG under Fault Conditions

A distribution system with DG under fault conditions was simulated to evaluate the current characteristics. The voltage drop improvement resulting from the presence of DG sizing of more than 3 MW connected at the middle point (M) was within the PEA voltage regulation. Thus, the DG sizing varied from 3 MW to 8 MW with three different DG placements: near the STA substation, at the middle of the distribution line, and near the SWA substation. In addition, the single-line to ground fault location varied among six locations along the distribution line in a manner similar to the case without DG. The single-line diagram and PSCAD model are shown in Figure 12a,b, respectively.

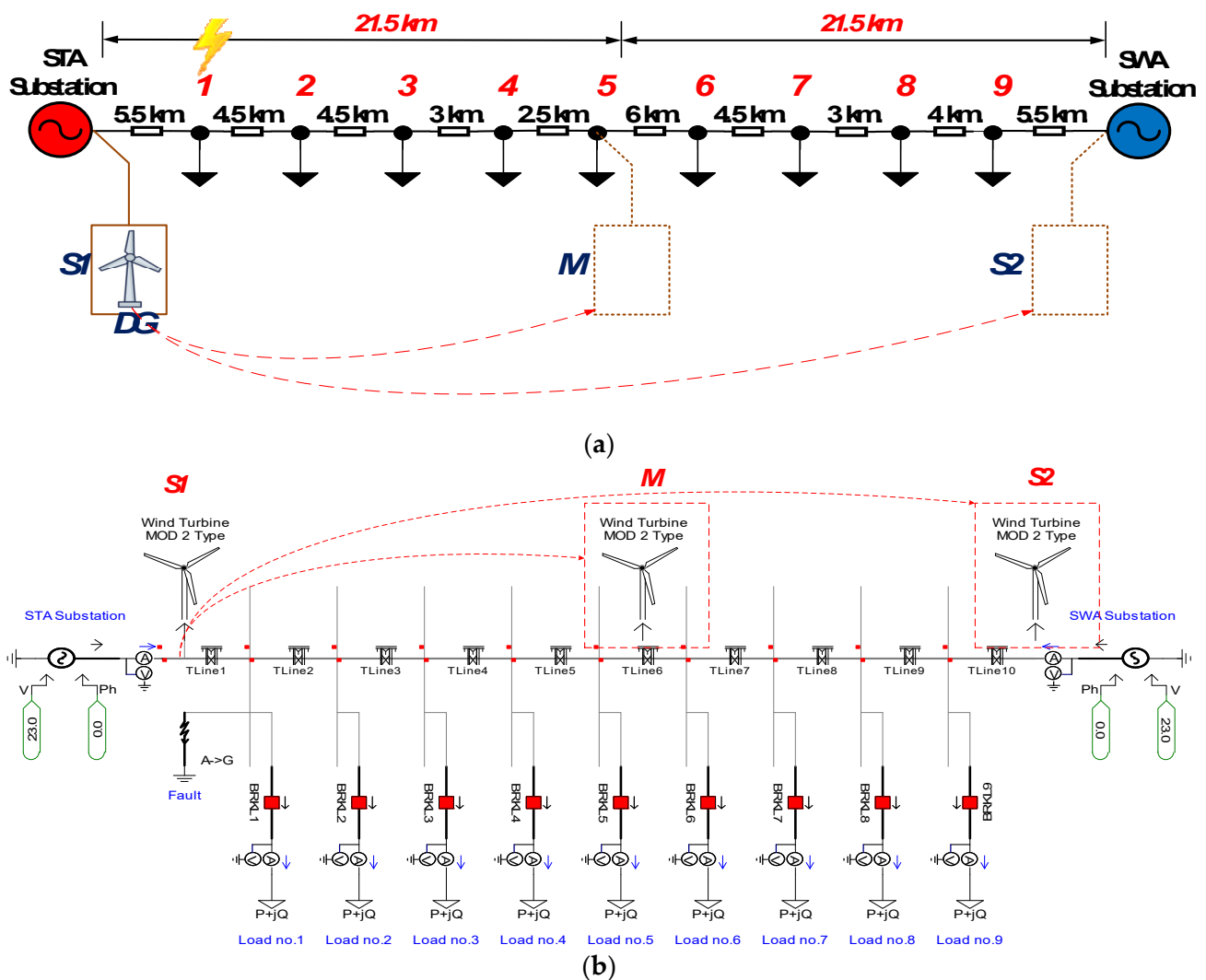


Figure 12. Distribution system with single DG placement under fault condition. (a) Single-line diagram; (b) PSCAD diagram.

The sinusoidal current waveforms from the STA substation, DG connected point, and SWA substation in the cases of single-phase fault to ground and three-phase fault to ground at location L1 are shown in Figure 13a,b, respectively. As shown, the location of the fault was near the STA substation, resulting in the current amplitude after fault occurrence being significantly higher when compared to the SWA substation. The current from the DG at the middle of the distribution line in the phase fault slightly increased compared to that in the pre-fault condition. However, the amplitude did not sharply increase, owing to the limitation of the current generated by the WTG.

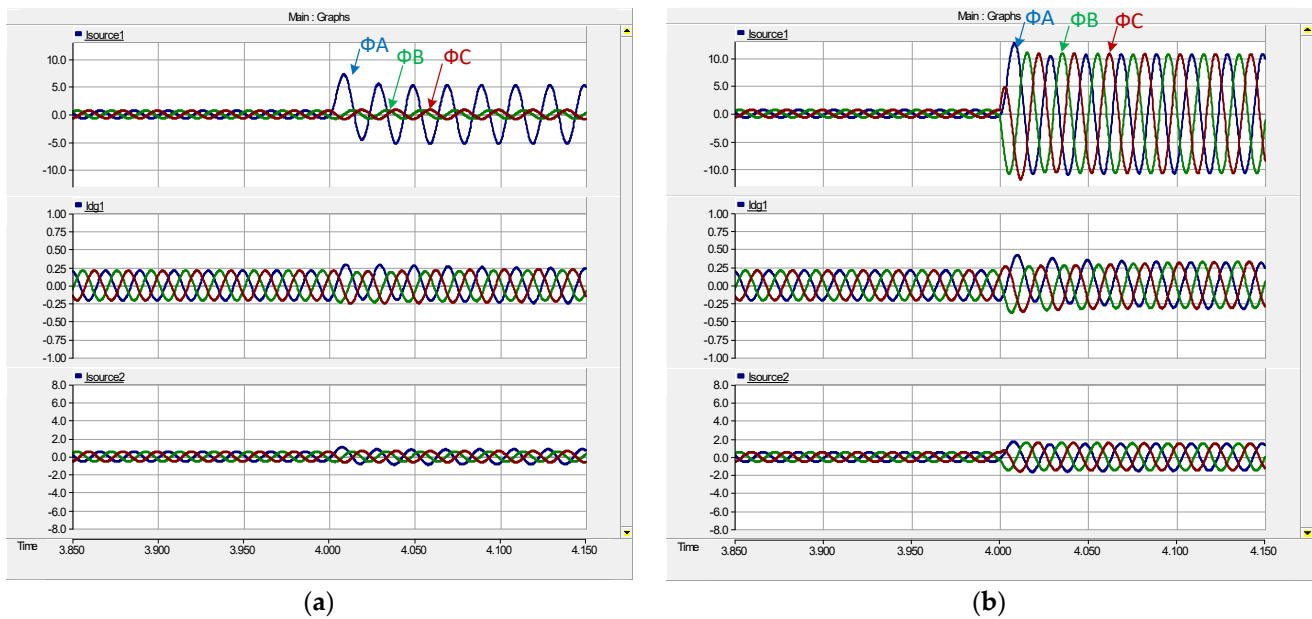


Figure 13. Current waveform at the fault location at 5.5 km with DG placed at the middle of the distribution system. (a) Single-phase fault to ground; (b) three-phase fault to ground.

4.3. Distribution System in the Case of Single DG under Various Fault Locations

The results from simulating the distribution system with a connected 3 MW DG under various fault locations are summarized in Table 8. For fault position L1, the STA substation current in the fault phase in post-fault condition increased compared to that in the pre-fault condition. However, the amplitude was less than that in the case without DG under similar conditions. This resulted from the DG generating additional power and current into the fault location. The SWA substation current also had a similar characteristic but was less affected by the presence of DG, which allowed the current from the SWA substation to flow through to the nearest load. The current on the load bus near the fault location decreased because of the current flow to the fault position. On the other hand, the load located far away from fault position and between the DG and the SWA substations was less affected by the decreasing current. This characteristic was caused by a similar resistance path between the load and fault positions in which the DG generated current and flowed both ways, and the SWA substation current could load the bus in-between.

When the fault location moved away from the STA substation to the location near the middle of the distribution line in which the DG was located, the post-fault current from the STA substation decreased and that in the SWA substation increased. In addition, the load bus current near the fault location decreased. This change was not similar to the case without DG. In the case in which the fault occurred between the DG and the SWA substations, the opposite occurred compared to the fault position at L1. This characteristic is similar to the main post-fault current originating from the SWA substation and DG. This result demonstrates that the current level and flow are altered when DG is present during a fault occurrence, and the position of the fault also significantly effects the characteristics.

Table 8. Current characteristics in the case of a distribution system with 3 MW DG at the middle point (M) under varying fault locations.

Fault Location	Parameters	Measuring Points											
		STA (S1)	Load No. 1	Load No. 2	Load No. 3	Load No. 4	Load No. 5	Load No. 6	Load No. 7	Load No. 8	Load No. 9	SWA (S2)	
Normal Condition	RMS Current (kA)	A	0.462155	0.035898	0.190778	0.102424	0.241254	0.120776	0.039484	0.097338	0.122070	0.007628	0.372955
		B	0.462155	0.035898	0.190778	0.102424	0.241254	0.120776	0.039484	0.097338	0.122070	0.007628	0.372955
		C	0.462155	0.035898	0.190778	0.102424	0.241254	0.120776	0.039484	0.097338	0.122070	0.007628	0.372955
Fault at 5.5 km (L1)	RMS Current (kA)	A	3.350859	3.875873	0.049368	0.039561	0.117352	0.067317	0.027353	0.076529	0.102934	0.006947	0.550503
		B	0.509782	0.049651	0.234932	0.115791	0.259409	0.127304	0.040195	0.097321	0.121592	0.007610	0.373297
		C	0.569199	0.046875	0.239042	0.124110	0.287262	0.140970	0.044451	0.106379	0.130555	0.007932	0.428855
Fault at 10 km (L2)	RMS Current (kA)	A	1.969711	0.018456	2.636615	0.027950	0.086082	0.053203	0.024157	0.070917	0.097640	0.006758	0.630972
		B	0.520884	0.041206	0.251161	0.121614	0.268988	0.131079	0.040847	0.098137	0.122272	0.007629	0.389854
		C	0.591338	0.041413	0.249009	0.128351	0.296177	0.145131	0.045448	0.108213	0.132329	0.007991	0.441544
Fault at 17.5 km (L3)	RMS Current (kA)	A	1.218242	0.025997	0.092901	0.032938	2.142779	0.027515	0.015812	0.056099	0.083815	0.006267	0.829761
		B	0.519040	0.037207	0.207318	0.121206	0.307445	0.146750	0.043992	0.102758	0.126037	0.007755	0.410029
		C	0.583505	0.030340	0.225305	0.129308	0.317921	0.154032	0.047724	0.112414	0.136087	0.008125	0.458019
Fault at 20 km (L4)	RMS Current (kA)	A	1.217067	0.025970	0.092311	0.032283	2.141804	0.026847	0.015756	0.056206	0.083878	0.006265	0.828898
		B	0.522745	0.037207	0.207329	0.121361	0.306798	0.146636	0.044006	0.102680	0.126119	0.007755	0.407454
		C	0.587915	0.039346	0.225305	0.129355	0.317864	0.154004	0.047727	0.112475	0.136128	0.008128	0.460042
Fault at 33.5 km (L5)	RMS Current (kA)	A	0.694390	0.031997	0.151590	0.069843	0.144844	0.063071	0.012523	0.028027	0.053128	0.003845	1.889275
		B	0.476797	0.035832	0.191145	0.104663	0.252375	0.130098	0.047069	0.125118	0.160301	0.008902	0.412728
		C	0.530858	0.037564	0.207296	0.115419	0.277644	0.141896	0.048297	0.124230	0.158084	0.008812	0.466108
Fault at 37.5 km (L6)	RMS Current (kA)	A	0.632474	0.032714	0.158713	0.075744	0.162303	0.073428	0.016677	0.028405	0.031145	3.790341	3.278373
		B	0.465596	0.035805	0.190499	0.103811	0.248799	0.127528	0.045330	0.118906	0.156489	0.010595	0.410326
		C	0.519209	0.037301	0.204732	0.113329	0.272003	0.138420	0.046848	0.119672	0.154281	0.010004	0.456568

4.4. Distribution System in the Case of Various Single DG Sizing under Fault Conditions

The DG connected allowance based on the PEA interconnection code is up to 8 MW. Thus, the effect of the DG sizing on the current characteristics needs to be evaluated. The simulation result from the fixed fault location at L1 when varying the DG sizing from 3 MW to 8 MW is shown in Figure 14. From Figure 14a–f, it can be seen that increasing the DG size resulted in lower STA and SWA substation currents, owing to the larger generating capacity from the DG. The current on the load bus increased slightly because of the proximity of the DG location and the reduction in loss from the line impedance. During fault conditions, a larger-capacity DG can generate more power and current to the fault position, while the load requires the same amount of power. This results in a decrease in the SWA substation current located far from the fault location. However, the current from the STA substation still increased with DG sizing because of the vicinity of the fault location. The current on the load bus increased as the DG sizing increased as a result of the ability of the DG to supply both the load and fault positions.

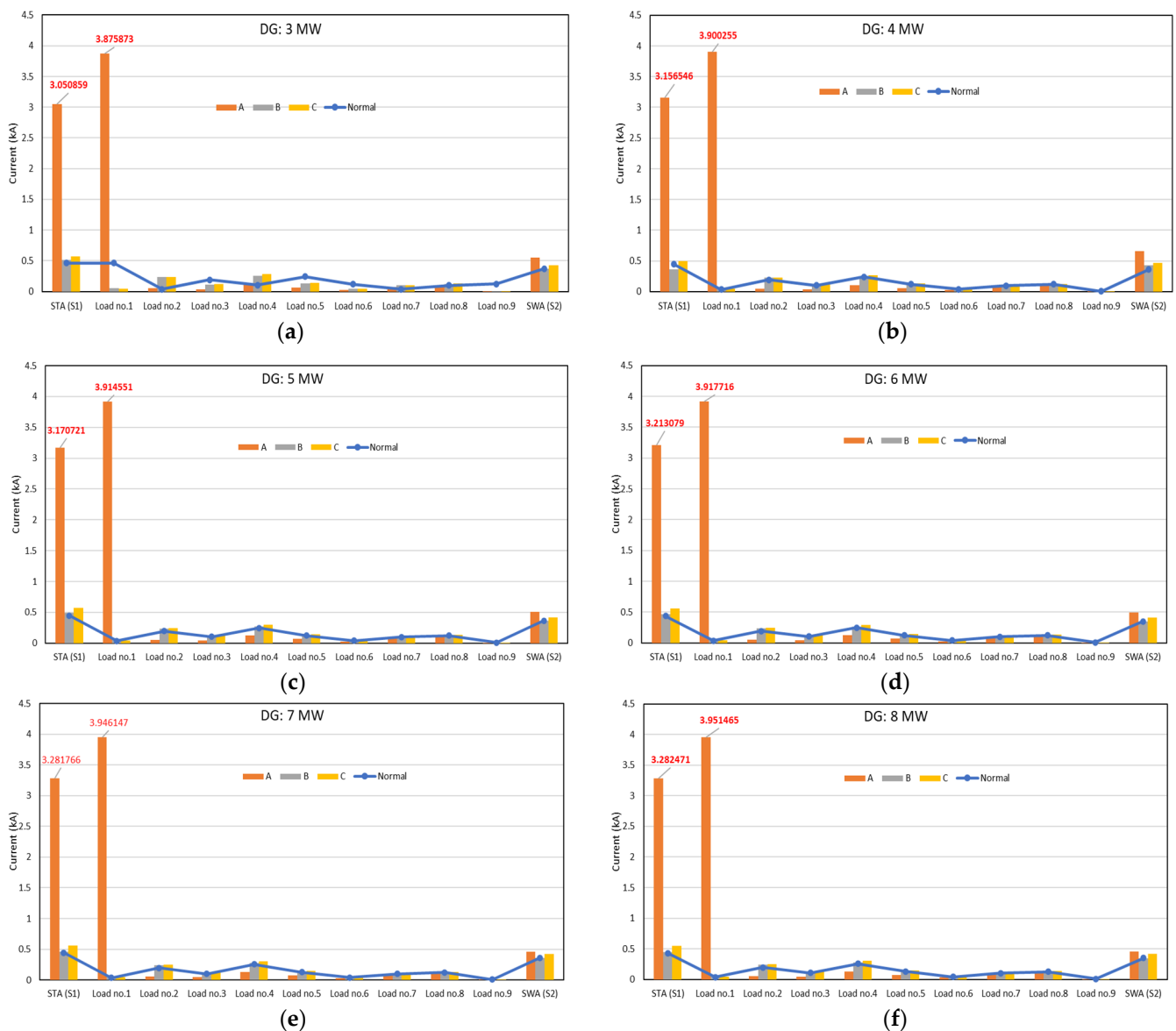


Figure 14. Current characteristics of the fixed fault location at L1 from 3 MW to 8 MW. (a) The 3 MW DG; (b) 4 MW DG; (c) 5 MW DG; (d) 6 MW DG; (e) 7 MW DG; and (f) 8 MW DG.

In conclusion, DG placement in the distribution system has an impact on the characteristics of the system under both normal and fault conditions. The flow of the current and amplitude levels depends on the DG and fault location. This is because the DG provides current to the fault position as an additional source on the distribution line. For the DG sizing, despite the current on substation decreasing and load bus increasing for the increased DG sizing, the overall characteristic of the system showed a similar pattern, and the sizing of DG did not impact the flow. However, a protection device that relies on the current level setting may have a significant impact.

5. Conclusions

This study aimed to investigate the effect of DG using WTG as a source on a distribution system under both normal and fault conditions that were analyzed. The WTG sizing varied between 2 MW–8 MW at three different locations: near the STA substation (S1), at the middle of the distribution line (M), and near the SWA substation (S2). The voltage level results showed that under normal conditions, DG connected to the distribution line can improve the voltage on all loads connected to the distribution line. The voltage level increases in proportion with DG sizing. The result found that DG with a size of 3 MW placed on the middle of the transmission line can improve voltage levels within the PEA voltage regulation limits with the maximum DG connection allowance reaching 8 MW, thus showing that the voltage level still did not go over the authoritative boundary. In the case of fault conditions without DG, the current flowed from the substation to the fault location instead of the load bus. However, DG placement can affect the direction of the current flow and provide the nearest load bus with current and power depending on the distance between the DG and the fault location. The current amplitude provided to the fault location was proportional to the sizing of the DG. However, this study only focused on wind power generation (WTG) based on a PEA 22 kV voltage level. The system characteristics may differ in the case of changing types of DG or voltage levels, suggesting that further analysis needs to be done. These impacts on the distribution system caused by DG can affect the operation of conventional distribution systems. With an increase in the DG penetration level, a new suitable operation must be considered to ensure good system reliability. Future work will compare DG with the high voltage capacitor bank regarding aspects of voltage improvement and provide recommendations for suitable devices to reduce voltage drop in distribution systems. Furthermore, a protection device will also be provided and studied.

Author Contributions: Conceptualization, A.N.; methodology, S.Y.; software, W.K.; validation, S.Y.; formal analysis, W.K.; investigation, W.K.; resources, I.N.; data curation, I.N.; writing—original draft preparation, W.K.; writing—review & editing, A.N.; visualization, S.Y.; supervision, I.N.; project administration, A.N.; funding acquisition, I.N. All authors have read and agreed to the published version of the manuscript.

Funding: This project was funded by the National Research Council of Thailand.

Institutional Review Board Statement: Not applicable.

Informed Consent Statement: Not applicable.

Data Availability Statement: Data sharing not applicable.

Acknowledgments: The authors wish to gratefully acknowledge financial support for this research from the National Research Council of Thailand.

Conflicts of Interest: The authors declare no conflict of interest.

References

1. Sanamehreen, M.; Binal, M.; Divyesh, M. Grid Integration of Distributed Generation: Issues and Challenges. In Proceedings of the 2022 International Conference for Advancement in Technology (ICONAT), Goa, India, 21–22 January 2022; pp. 1–6.
2. Ministry of Energy. *Thailand Power Development Plan 2018–2037 (PDP 2018 Revision 1)*; Ministry of Energy: Bangkok, Thailand, 2020. Available online: https://www.eppo.go.th/images/Infomation_service/public_relations/PDP2018/PDP2018Rev1.pdf (accessed on 20 October 2020).

3. Ministry of Energy. *Alternative Energy Development Plan 2018–2037 (AEDP 2018)*; Ministry of Energy: Bangkok, Thailand, 2020. Available online: https://www.dede.go.th/download/Plan_62/20201021_TIEB_AEDP2018.pdf (accessed on 20 October 2020).
4. Laura, M.; Deane, P.; Gallachóir, B.; Bertsch, V. A review of the role of distributed generation (DG) in future electricity systems. *Energies* **2018**, *163*, 822–836.
5. Toloo, M.; Taghizadeh-Yazdi, M.; Mohammadi-Balani, A. Multi-objective centralization-decentralization trade-off analysis for multi-source renewable electricity generation expansion planning: A case study of Iran. *Comput. Ind. Eng.* **2022**, *164*, 107870.
6. ChithraDevi, S.A.; Lakshminarasimman, L.; Balamurugan, R. Stud Krill herd Algorithm for multiple DG placement and sizing in a radial distribution system. *Eng. Sci. Technol. Int. J.* **2017**, *20*, 748–759. [[CrossRef](#)]
7. Nawaz, S.; Tandon, A. A New Technique to Solve Dg Allocation Problem for Distribution Power Loss Minimization. *ICIC Express Lett. Part B Appl. Int. J. Res. Surv.* **2018**, *9*, 701–706.
8. Alok, K.B.; Venkataramana, A. Investigation of Relevant Distribution System Representation with DG for Voltage Stability Margin Assessment. *IEEE Trans. Power Syst.* **2020**, *35*, 2072–2081.
9. Suresh, M.C.V.; Edward, J.B. A hybrid algorithm based optimal placement of DG units for loss reduction in the distribution system. *Appl. Soft Comput.* **2020**, *91*, 106191. [[CrossRef](#)]
10. Muhammad, M.A.; Chuangxin, G.; Muhammad, S.S.; Munsif, A.J.; Caiming, Y.; Jianguang, Z. A Review of Technical Methods for Distributed Systems with Distributed Generation (DG). In Proceedings of the 2019 2nd International Conference on Computing, Mathematics and Engineering Technologies (iCoMET), Sukkur, Pakistan, 30–31 January 2019; pp. 1–7.
11. Iqbal, F.; Khan, M.T.; Siddiqui, A.S. Optimal placement of DG and DSTATCOM for loss reduction and voltage profile improvement. *Alex. Eng. J.* **2018**, *57*, 755–765.
12. Pankita, M.; Praghness, B.; Vivek, P. Optimal selection of distributed generating units and its placement for voltage stability enhancement and energy loss minimization. *Ain Shams Eng. J.* **2018**, *9*, 187–201.
13. Paschalis, A.G.; Aggelos, S.B.; Dimitrios, I.D.; Kallisthenis, I.S.; Dimitris, P.L. Load variations impact on optimal DG placement problem concerning energy loss reduction. *Electr. Power Syst. Res.* **2017**, *152*, 36–47.
14. Haijun, X.; Xin, S. Distributed Generation Locating and Sizing in Active Distribution Network Considering Network Reconfiguration. *IEEE Access.* **2017**, *5*, 14768–14774.
15. Sirine, E.; Adel, B.; Adel, K. Optimal Sizing and Placement of DG Units in Radial Distribution System. *Int. J. Renew. Energy Res.* **2018**, *8*, 167–177.
16. Alwash, S.F.; Ramachandaramurthy, V.K.; Mithulanathan, N. Fault-Location Scheme for Power Distribution System with Distributed Generation. *IEEE Trans. Power Deliv.* **2015**, *30*, 1187–1195. [[CrossRef](#)]
17. Mohsin, S.; Waseem, A.; Muhammad, A.; Uzair, K.; Barkat, U. Optimal Siting and Sizing of Distributed Generators by Strawberry Plant Propagation Algorithm. *Energies* **2021**, *14*, 3–13.
18. Ali, T.; Faissal, E.; Abdelaziz, B.; Touria, H.; Naima, A.; Rabiaa, G. Meta-heuristics Applied to Multiple DG Allocation in Radial Distribution Network: A comparative study. In Proceedings of the 2022 International Conference on Intelligent Systems and Computer Vision (ISCV), Fez, Morocco, 18–20 May 2022; pp. 1–8.
19. Mohammad, I.; Mohsin, S.; Noman, U. Analytical Method for Optimal Reactive Power Support in Power Network. In Proceedings of the 2019 2nd International Conference on Computing, Mathematics and Engineering Technologies (iCoMET), Sukkur, Pakistan, 30–31 January 2019; pp. 1–6.
20. Chiradeja, P.; Yoomak, S.; Ngaopitakkul, A. The study of economic effects when different distributed generators (DG) connected to a distribution system. In Proceedings of the 2018 19th International Scientific Conference on Electric Power Engineering (EPE), Brno, Czech Republic, 16–18 May 2018; pp. 1–5.
21. Ngaopitakkul, A.; Jettanasen, C. The effects of multi-distributed generator on distribution system reliability. In Proceedings of the 2017 IEEE Innovative Smart Grid Technologies—Asia (ISGT-Asia), Auckland, New Zealand, 4–7 December 2017; pp. 1–6.
22. Hany, F.H.; Nevin, F.; Mohammad, M.E.; Osama, A.M. Enhancement of Protection Scheme for Distribution System Using the Communication Network. In Proceedings of the 2019 IEEE Industry Applications Society Annual Meeting, Baltimore, MD, USA, 29 September–3 October 2019; pp. 2–7.
23. Digambar, R.B.; Ravishankar, S.K.; Saurabh, J. Impact of Distributed Generation on Protection of Power System. In Proceedings of the 2017 International Conference on Innovative Mechanisms for Industry Applications (ICIMIA), Bengaluru, India, 21–23 February 2017; pp. 399–405.
24. Langlang, G.; Muhammad, A.H.; Mokhammad, S.; Wahyu, S.N. Analysis of Short Circuit on Four Types Wind Power Plants as Distributed Generation. In Proceedings of the 2020 International Conference on Smart Technology and Applications (ICoSTA), Surabaya, Indonesia, 20 February 2020; pp. 1–6.
25. Mehdi, M.; Matin, M.; Abbas, F. Impact of Size and Location of Distributed Generation on Overcurrent Relays in Active Distribution Networks. In Proceedings of the 2017 North American Power Symposium (NAPS), Morgantown, WV, USA, 17–19 September 2017; pp. 1–6.
26. Reza, M.C.; Ehsan, M.H.; Meysam, F. The effect of fault current limiter size and type on current limitation in the presence of distributed generation. *Turk. J. Electr. Eng. Comput. Sci.* **2017**, *25*, 1021–1034.
27. Adel, A.A.E.; Ragab, A.E.; Abdullah, M.S.; Aya, R.E. Optimal Allocation of Distributed Generation Units Correlated with Fault Current Limiter Sites in Distribution Systems. *IEEE Syst. J.* **2021**, *15*, 2148–2155.

28. Mir, E.H.; Reza, M.C. Optimal Allocation of Distributed Generation with Optimal Sizing of Fault Current Limiter to Reduce the Impact on Distribution Networks Using NSGA-II. *IEEE Syst. J.* **2019**, *13*, 1714–1724.
29. Matin, M.; Alexander, D.; Ilya, G. Impact of distributed generation on the protection systems of distribution networks: Analysis and remedies—Review paper. *IET Gener. Transm. Distrib.* **2020**, *14*, 5944–5960.
30. Ayoade, F.A.; Owolabi, B.; Ademola, A.; Ayokunle, A.; Tobiloba, S.; Akinola, O.; Agbetuyi, O. Investigation of the Impact of Distributed Generation on Power System Protection. *Adv. Sci. Technol. Eng. Syst. J.* **2021**, *6*, 324–331.
31. Hamid, M.; Rahman, D.; Ahmad, K.; Amin, J.T.; Hamid, R.S. A Novel Fault Location Methodology for Smart Distribution Networks. *IEEE Trans. Smart Grid* **2021**, *12*, 1277–1288.
32. Gustavo, G.S.; José Carlos, M.V. Optimal Placement of Fault Indicators to Identify Fault Zones in Distribution Systems. *IEEE Trans. Power Deliv.* **2021**, *36*, 3282–3285.
33. Haotian, S.; Hao, Y.; Fang, Z.; Xiaotong, D.; Guangyu, Y. Precise Fault Location in Distribution Networks Based on Optimal Monitor Allocation. *IEEE Trans. Power Deliv.* **2020**, *35*, 1788–1799.
34. Farzaneh, S.; Mohammad, R.; Morteza, D. Simultaneous Placement of Tie-lines and Distributed Generations to Optimize Distribution System Post-Outage Operations and Minimize Energy Losses. *CSEE J. Power Energy Syst.* **2021**, *7*, 318–328.
35. Liuzhu, Z.; Bin, Y.; Xijun, R.; Bao, W.; Xiaoyu, S.; Mao, Z.; Pei, Z.; Xiaoxi, L.; Jiateng, L. Transmission Pricing for Distributed Generation Transactions Based on Cost and Benefit Analysis. In Proceedings of the 2020 IEEE 4th Conference on Energy Internet and Energy System Integration (EI2), Wuhan, China, 30 October–1 November 2020; pp. 4397–4402.
36. Bangun, N.; Kamaruddin, A.; Aep, S.U.; Erkata, Y.; Syukri, M.N.; Herry, S.; Zane, V.; Roy, H.S.; Yanuar, N. Smart Micro-Grid Performance using Renewable Energy. *ICESTI* **2019**, *188*, 1–11.

Disclaimer/Publisher’s Note: The statements, opinions and data contained in all publications are solely those of the individual author(s) and contributor(s) and not of MDPI and/or the editor(s). MDPI and/or the editor(s) disclaim responsibility for any injury to people or property resulting from any ideas, methods, instructions or products referred to in the content.